conjugated horse anti-rabbit IgG antibody (1:10 000). Glyceraldehyde 3-phosphate dehydrogenase (GAPDH) was used as an internal control for the brain tissues. Immunoreactivity was detected by enhanced chemiluminescence autoradiography (ECL™ western blotting detection kit; Amersham Pharmacia Biotech, Uppsala, Sweden), and the film was analysed using the public domain software NIH Image (developed at the US National Institutes of Health and available on the Internet at http://rsb.info.nih.gov/nih-image/).

2.8.2 *Reverse transcriptase PCR*

Total RNA was prepared from the circumventricular tissues including hypothalamus using RNAlater solution (Ambion, Austin, TX, USA). Complementary DNAs were synthesized by standard techniques using a ReverTra Ace qPCR RT Kit (TOYOBO, Osaka, Japan). Real-time PCR was performed, recorded, and analysed using a thermal cycler dice real-time system (Takara Bio, Shiga, Japan) with SYBR Green I detection. cDNA was amplified using a SYBR Premix Ex Taq (Perfect Real Time) PCR kit (Takara Bio) with specific primers (Sigma R1, forward: 5′-CTC GCT GTC TGA GTA CGT G-3′; reverse: 5′-AAG AAA GTG TCG GCT AGT GCA A-3′; HPRT1, forward: 5′-GCG TCG TGA TTA GCG ATG ATG AAC-3′; reverse: 5′-CCT CCC ATC TCC TCC ATG ACA TCT-3′). HPRT1 was used as a reference to normalize the amount of total RNA amplified in each reaction. Relative gene expression data were analysed using the 2 $(-\Delta\Delta CT)$ method.[27]

2.9 Evaluation of the depression-like behaviour index

Depression was evaluated by the tail suspension test, which uses increased immobility time as an index of depression-like behaviour in mice.[28] Tail suspension was conducted in a force transducer, and strain amplitude data were also recorded using the Powerlab system as a marker of struggle activity. The test was performed in the afternoon, and immobility time and struggle activity were determined during 6-min recordings. Additionally, locomotor activity was evaluated by a digital actophotometer.[29] Two mice were placed in the actophotometer apparatus cage, and the total number of ambulatory movements was scored over 24 h. The daily variation of locomotor activity was also evaluated by the ratio of movement scores from night to day.

2.10 Measurement of serum and brain DHEAS

Under anaesthesia with an overdose of sodium pentobarbital, a blood sample was collected from the right ventricle, and the mice were perfused with distilled H_2O. After adequate perfusion to remove blood, the brain circumventricular tissues and hypothalamus were dissected out. The tissues (0.10 g) were homogenized in 200 μL distilled H_2O, rapidly centrifuged, and the supernatant was collected.[18] DHEAS concentration was measured by enzyme-linked immunosorbent assay (ELISA).

2.11 Statistical analysis

All values are expressed as mean ± SE. Analysis of variance was used to compare U-NE, organ weight, LVDD, LVSD, LVWT, %FS, immobility time, strain amplitude, DHEAS concentration, mRNA levels, and protein levels between groups. An unpaired *t*-test was used to compare locomotor activity between Sham and AB-H and changes in protein levels between mice treated with and without S1R ligands. Differences were considered significant at $P < 0.05$.

3. Results

3.1 Characteristics of AB-H

Both relative heart weight (heart weight/body weight) and absolute heart weight were greater in AB-H than Sham (relative heart weight: Sham, 4.87 ± 0.05 mg/g; AB-H, 6.45 ± 0.08 mg/g, absolute heart weight: Sham, 0.23 ± 0.02 g; AB-H, 0.26 ± 0.05 g; $P < 0.05$, $n = 8$ per group). Relative lung weight (lung weight/body weight) tended to increase in AB-H compared with Sham (Sham, 5.81 ± 0.15mg/g; AB-H, 6.20 ± 0.09 mg/g; $n = 8$ per group). The body weight of AB-H was significantly lower than that of Sham (Sham, 47.4 ± 0.8 g; AB-H, 40.6 ± 1.1 g; $P < 0.05$, $n = 8$ per group). Echocardiography revealed that LV dimensions and LVWT were greater in AB-H than Sham, and %FS was significantly lower in AB-H than Sham (*Figure 1*). Sympathetic activity evaluated by U-NE excretion was increased in AB-H compared with Sham (Sham, 350 ± 44 ng/day; AB-H, 731 ± 26 ng/day; $P < 0.05$, $n = 8$ per group). In Sham, HS intake did not alter body weight, organ weight, cardiac function, or sympathetic activity (Sham vs. Sham-H). Mean BP was lower and the heart rate was higher in AB-H than Sham (mean BP: Sham, 90 ± 2 mmHg; AB-H, 78 ± 1 mmHg, heart rate: Sham, 422 ± 16 b.p.m.; AB-H, 477 ± 14 b.p.m.; $P < 0.05$, $n = 5$ per group). Tail suspension test revealed increased immobility time and decreased strain amplitude in AB-H compared with Sham (*Figure 2A–C*). Locomotor activity (24 h) was lower in AB-H than Sham (Sham, 7387 ± 459 counts; AB-H, 3877 ± 864 counts; $P < 0.05$, $n = 6$ per group), and the ratio of locomotor activity during night to day, a marker of daily variation, was smaller in AB-H than Sham (Sham, 3.2 ± 0.6; AB-H, 1.6 ± 0.1; $P < 0.05$, $n = 6$ per group).

3.2 S1R expression in the brain

The protein levels of brain S1R were decreased in AB-H compared with Sham. In Sham, HS intake did not alter those levels (*Figure 3*). The mRNA levels of brain S1R did not significantly alter between Sham and AB-H (Sham, 1.2 ± 0.1; AB-H, 0.9 ± 0.1; $n = 5$ per group).

3.3 Effects of acute PRE084 ICV infusion on cardiovascular regulation

ICV infusion of PRE084 lowered heart rate in both AB-H and Sham. However, changes in the heart rate were significantly smaller in AB-H than in Sham (*Figure 4A*). Furthermore, sympathetic activity evaluated by power spectral analysis of SBP was decreased significantly only in Sham (*Figure 4B*).

3.4 Effects of chronic PRE084 ICV infusion

Chronic ICV infusion of PRE084 (PRE) increased protein levels of brain S1R in AB-H compared with no treatment (*Figure 5A*). mRNA levels of brain S1R slightly increased after chronic PRE084 ICV infusion (AB-H, 0.9 ± 0.1; AB-H with PRE, 1.3 ± 0.1; $P < 0.05$, $n = 5$ per group). Chronic PRE084 ICV infusion lowered the enhanced sympathetic activity (AB-H, 731 ± 26 ng/day; AB-H with PRE, 571 ± 43 ng/day; $P < 0.05$, $n = 8$ and 5, respectively) and improved cardiac function in AB-H compared with no treatment (*Figure 5B*). Furthermore, PRE084 also decreased both relative heart weight (heart weight/body weight) and absolute heart weight compared with no treatment (relative heart weight: AB-H, 6.45 ± 0.08 mg/g; AB-H with PRE, 4.50 ± 0.15 mg/g, absolute heart weight: AB-H, 0.26 ± 0.05 g; AB-H with PRE, 0.19 ± 0.07 g; $P < 0.05$, $n = 8$ and 5, respectively). Chronic ICV infusion of PRE084 decreased immobility time and increased strain amplitude in AB-H compared with no treatment (*Figure 5C*).

Downloaded from http://cardiovascres.oxfordjournals.org/ by guest on May 10, 2012

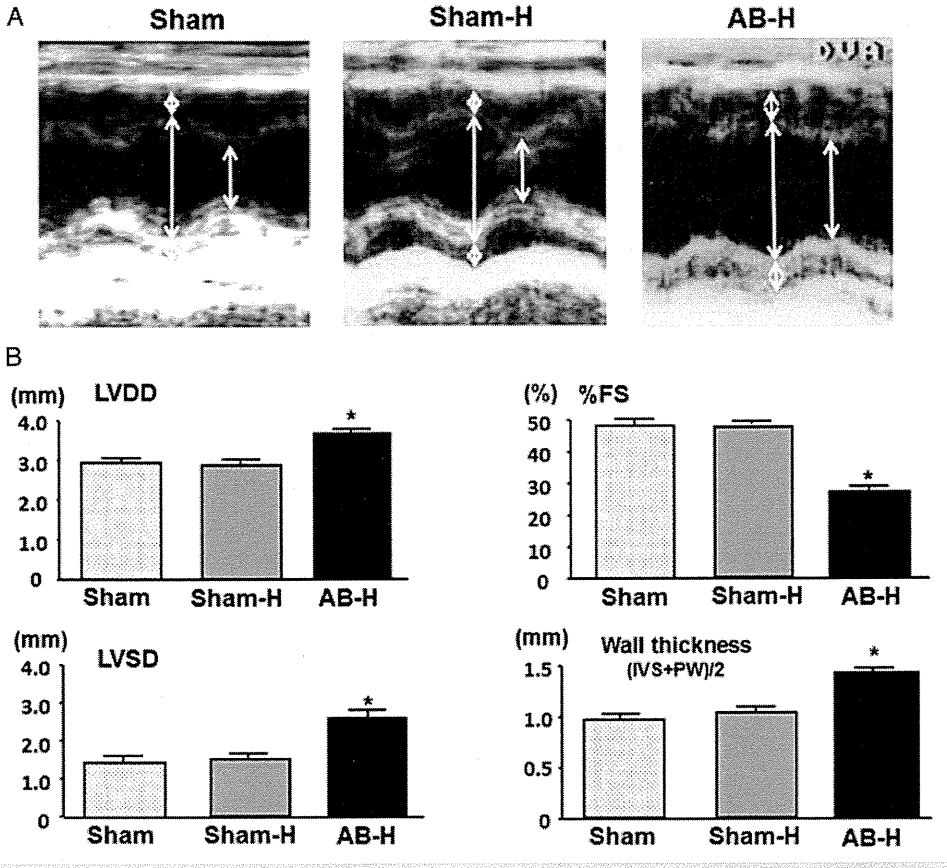

Figure 1 (*A*) Representative M-mode echocardiography. (*B*) Cardiac function evaluation by echocardiography. *$P < 0.05$ vs. Sham and Sham-H ($n = 8$ per group). LVDD, left ventricular end-diastolic diameter; LVSD, left ventricular end-systolic diameter; %FS, per cent fractional shortening; IVS, interventricular septum; PW, posterior wall.

3.5 Effects of chronic oral administration of fluvoxamine

Chronic oral administration of fluvoxamine lowered enhanced sympathetic activity (AB-H, 731 ± 26 ng/day; AB-H with fluvoxamine, 561 ± 20 ng/day; $P < 0.05$, $n = 8$ and 5, respectively) and improved cardiac function compared with no treatment (%FS: AB-H, 27 ± 2%; AB-H with fluvoxamine 37 ± 3%; $P < 0.05$, $n =$ 8 and 5, respectively). Chronic oral administration of fluvoxamine decreased immobility time and increased strain amplitude compared with no treatment (immobility time: AB-H, 162 ± 9 s; AB-H with fluvoxamine, 93 ± 10 s; strain amplitude: AB-H, 0.12 ± 0.01; AB-H with fluvoxamine, 0.19 ± 0.02; both $P < 0.05$, $n = 15$ and 5, respectively).

3.6 Effects of chronic BD1063 ICV infusion on characteristics of Sham mice

Chronic ICV infusion of BD1063 (BD)-enhanced sympathetic activity (24-h U-NE excretion: Sham, 350 ± 44 ng/day; Sham with BD, 576 ± 25 ng/day; $P < 0.05$, $n = 8$ and 5, respectively) and tended to impair cardiac function compared with no treatment (%FS: Sham, 47 ± 2%; Sham with BD, 40 ± 3%; $P < 0.05$, $n = 8$ and 5, respectively).

3.7 DHEAS concentration

Serum DHEAS concentrations were lower in AB-H compared with Sham or Sham-H (Sham, 0.039 ± 0.009 μg/mL; Sham-H, 0.040 ± 0.006 μg/mL; AB-H, 0.013 ± 0.008 μg/mL; $P < 0.05$, $n = 5$ per group). Brain DHEAS concentrations were also lower in AB-H compared with Sham or Sham-H (Sham, 0.047 ± 0.001 μg/mL; Sham-H, 0.046 ± 0.002 μg/mL; AB-H, 0.033 ± 0.005 μg/mL; $P < 0.05$, $n = 5$ per group).

4. Discussion

The present study demonstrates that in AB-H (i) cardiac function decreased with enhanced sympathetic activity; (ii) brain S1R expression decreased; (iii) the index of depression-like behaviour was higher compared with Sham; (iv) the decrease in sympathetic activity and the heart rate in response to acute ICV infusion of PRE084, a selective S1R agonist, was smaller compared with Sham; and (v) chronic ICV infusion of PRE084 increased brain S1R expression, lowered enhanced sympathetic activity, and improved cardiac function and the index of depression-like behaviour. These findings indicate that the reduction in brain S1R expression in AB-H contributed to both the exacerbation of cardiac dysfunction via enhanced sympathetic activity and the worsening of depression.

Downloaded from http://cardiovascres.oxfordjournals.org/ by guest on May 10, 2012

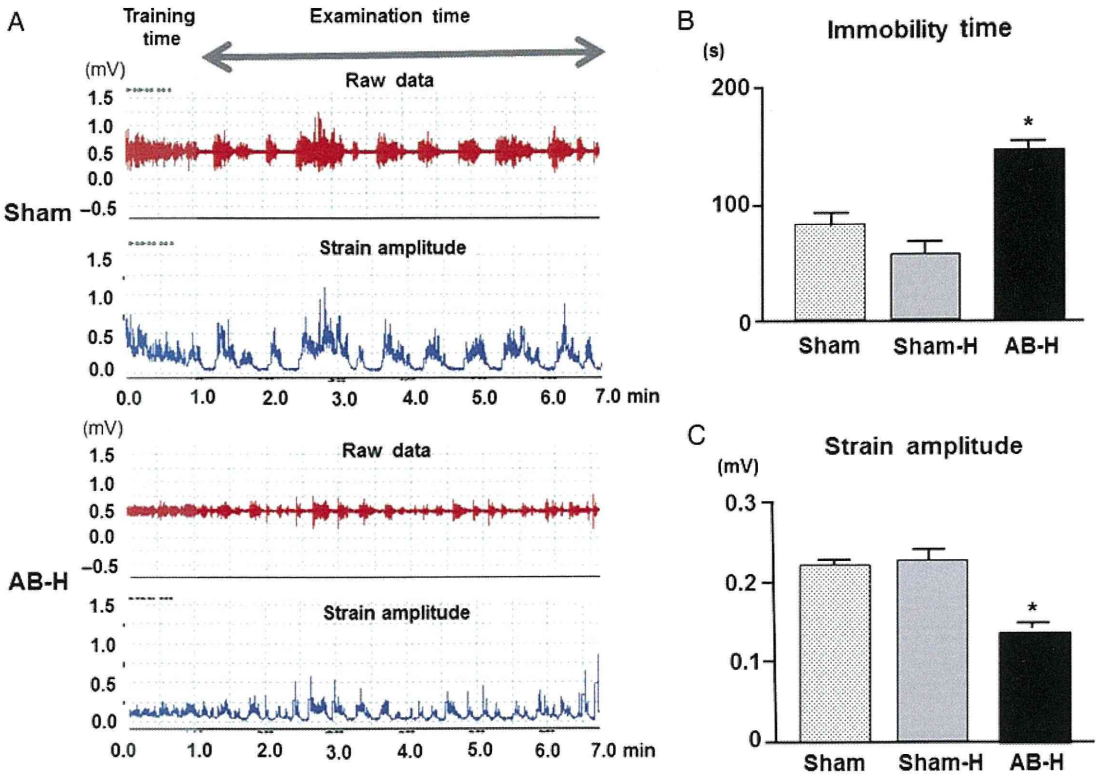

Figure 2 (*A*) Representative recordings of strain amplitude in the tail suspension test from Sham (upper) and AB-H (lower). (*B* and *C*) Grouped data of immobility time (*B*) and strain amplitude (*C*) in Sham and AB-H. *$P < 0.05$ vs. Sham (Sham and Sham-H, $n = 13$; AB-H, $n = 15$).

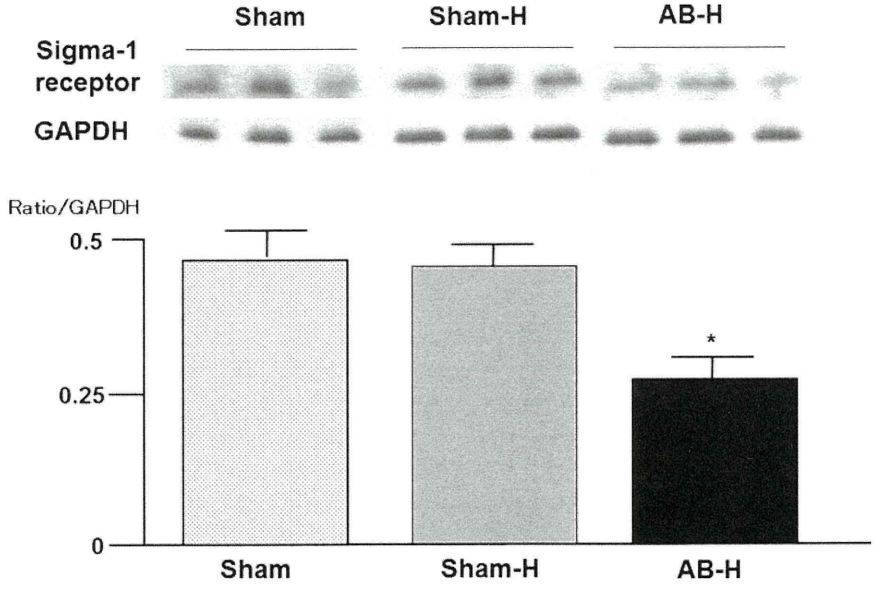

Figure 3 Representative western blots demonstrating the expression of S1R in the brain. The graph shows the means for the quantification of three separate experiments. Data are expressed as the relative ratio of GAPDH expression. *$P < 0.05$ vs. Sham and Sham-H. GAPDH, Glyceraldehyde 3-phosphate dehydrogenase.

Downloaded from http://cardiovascres.oxfordjournals.org/ by guest on May 10, 2012

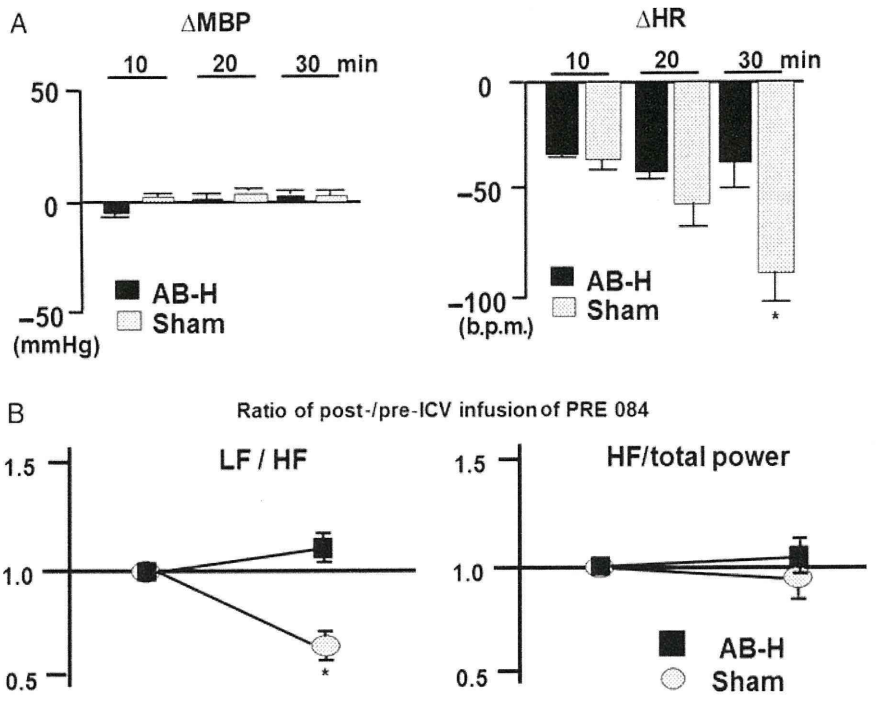

Figure 4 (*A*) Grouped data of MBP and HR response to ICV infusion of PRE084 in Sham and AB-H mice. *X*-axis (10, 20, 30 min) indicates time after initiating PRE084 ICV infusion. $^*P < 0.05$ vs. AB-H ($n = 5$ per group). (*B*) Grouped data of LF/HF, as a marker of sympathetic activity, and HF/total power, as a marker of parasympathetic activity, in response to PRE084 ICV infusion. $^*P < 0.05$ vs. AB-H ($n = 5$ per group). MBP, mean blood pressure; HR, heart rate.

4.1 Reduction of brain S1R in AB-H mice

We demonstrated that the expression of brain S1R was decreased in AB-H and that this reduction was involved in the enhanced sympathetic activity. In AB-H, LV dimensions and LVWT increased, and %FS decreased with the enhanced sympathetic activity. We have previously confirmed the elevated LV end-diastolic pressure observed in this model.[18] Therefore, AB-H was used as a model for pressure-overload-induced heart failure. The protein levels of brain S1R were significantly decreased in AB-H, and ICV infusion of PRE084 decreased sympathetic activity and the heart rate to a greater extent in Sham than in AB-H. These results indicate that the protein levels of brain S1R and the S1R response to the receptor agonist were decreased in AB-H. The mRNA levels of brain S1R were also examined in the present study and found not to differ between Sham and AB-H, suggesting a higher turnover rate of S1R in AB-H.[30]

4.2 Depressive status in AB-H

We demonstrated that immobility time was increased in AB-H compared with Sham. In addition, a decrease in strain amplitude was confirmed as a marker of struggle activity in AB-H. AB-H had lower cardiac function compared with Sham, and the results of the tail suspension test may reflect exercise intolerance caused by cardiac dysfunction. However, short-term momentum in the home cage measured immediately after the test did not differ between AB-H and Sham (data not shown), suggesting that the results of the tail suspension test reflect the greater depressive status in AB-H, rather than exercise intolerance caused by cardiac dysfunction. Furthermore, the decreased 24-h locomotor activity and disappearance of daily variation of locomotor activity were confirmed in AB-H.

4.3 Effects of brain S1R stimulation

To clarify the importance of the reduction in brain S1R expression in this heart failure model, chronic ICV infusion of PRE084 in AB-H and BD1063 in Sham was performed. Chronic PRE084 ICV infusion increased brain S1R expression in AB-H. Our findings are compatible with those of previous studies, in which expression of the S1R was reported to increase in response to chronic agonist stimulation.[16] In addition, chronic PRE084 ICV infusion attenuated the enhanced sympathetic activity and improved cardiac function in AB-H. In contrast, chronic BD1063 ICV infusion enhanced sympathetic activity and tended to decrease cardiac function in Sham. ICV infusion of PRE084 also improved the index of depression-like behaviour in AB-H.

To our knowledge, no previous studies have reported chronic PRE084 or BD1063 infusion into the cerebrospinal fluid (CSF). PRE084 has an IC50 of 44 nM in the S1R and IC50 > 10 000 nM in a variety of other receptors.[21] BD1063 has nanomolar affinity for S1R and is 30-fold more selective for S1R than the sigma-2 receptor.[23] In the present study, the estimated concentration of both chemicals in the CSF was considered to be in the nanomolar range.[31] Therefore, the doses of both chemicals in the present study were adequate for use as specific S1R ligands. Using these doses, we were able to successfully show that the brain S1R plays an important role in modulating sympathetic activity and depressive status.

To clarify the effects of systemic treatment with S1R agonist, fluvoxamine, a potent agonist of S1R in addition to its function as a selective serotonin reuptake inhibitor, was orally administered.[19] The dose of fluvoxamine was determined according to a previous report.[19] Systemic administration of S1R agonist also attenuated the

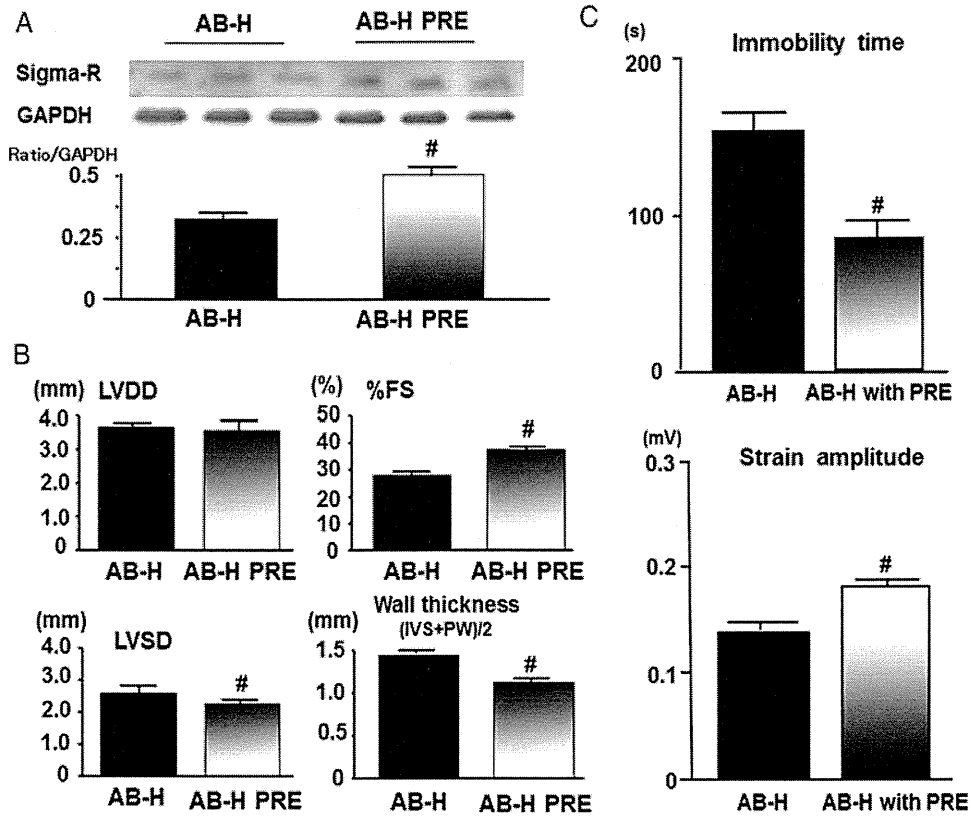

Figure 5 (*A*) Representative western blots demonstrating S1R expression in the brain after PRE084 ICV infusion in AB-H (AB-H with PRE). The graph shows the means for the quantification of three separate experiments. Data are expressed as the relative ratio of GAPDH expression. $^{\#}P < 0.05$ vs. AB-H. GAPDH, Glyceraldehyde 3-phosphate dehydrogenase. (*B*) Cardiac function evaluation by echocardiography after PRE084 ICV infusion in AB-H (AB-H with PRE). $^{\#}P < 0.05$ vs. AB-H (AB-H with PRE, $n = 5$; AB-H, $n = 8$). (*C*) Grouped data of immobility time and strain amplitude after PRE084 ICV infusion in AB-H (AB-H with PRE). $^{\#}P < 0.05$ vs. AB-H (AB-H with PRE, $n = 10$; AB-H, $n = 15$).

sympathetic hyperactivation in addition to improving depression-like behaviour.

The mechanisms involved in the modulation of sympathetic activity via the brain S1R remain unclear. The S1R is known to modulate neuronal intracellular calcium levels[13] and *N*-methyl-D-aspartate-mediated response.[14,15] Furthermore, S1R was reported to enhance brain plasticity and functional recovery after stroke.[32] These results suggest that the brain S1R affects neuronal activity and that the S1R in the central cardiovascular control region contributes to the regulation of sympathetic activity. Western blotting for brain S1R detection in circumventricular brain tissue including hypothalamus was performed. Wide distribution of the S1R has been reported in the brain, most abundantly in the hippocampus, facial nucleus, thalamus, and hypothalamus.[33] Therefore, the hypothalamus, one of the central cardiovascular control regions, is a promising candidate for the target nucleus involved in modulating sympathetic activity via the S1R. However, the S1R has also been reported in the brainstem, where the other cardiovascular control centre is located. ICV infusion of PRE084 or BD1063 possibly affected the S1R in the brainstem.

In addition, microglia releasing pro-inflammatory mediators such as cytokines and reactive oxygen species[34] also expresses high levels of S1R, and S1R suppresses microglial activation.[35] Such pro-inflammatory mediators in the brain were reported to cause sympathetic hyperactivation in models of heart failure.[36] Therefore, both neuronal and microglial S1R may be involved in the modulation of sympathetic activity.

4.4 Involvement of DHEAS in brain S1R reduction

The mechanisms involved in the reduction in brain S1R expression in this heart failure model also remain unclear. Neurosteroids, such as DHEA and its sulfate conjugate DHEAS, are recognized as endogenous S1R agonists.[14,16] DHEAS is produced mainly in adrenal tissues,[37] and its serum concentration was reported to decrease in heart failure patients.[17] In the present study confirmed that both serum and brain DHEAS concentrations decreased in AB-H compared with Sham mice. Furthermore, a recent study demonstrated that DHEAS deficiencies predicted the severity of depression in heart failure.[38] Therefore, a decrease in serum DHEAS concentration may have been responsible for the reduction in brain S1R expression observed in this heart failure model.

4.5 Limitations

The present study revealed that brain S1R expression decreased in AB-H, and the reduction in brain S1R may be involved in depression-like behaviour in this model. However, depression is a clinical syndrome that may have multi-pathogenetic causes. Therefore, other mechanisms may contribute to depression-like behaviour in this model. In fact, brain angiotensin type 1 receptor (AT1R) was reported to be a novel therapeutic approach for treatment of mood disorders via anti-inflammatory effects.[39] In previous studies, we confirmed that the brain AT1R increased in AB-H.[18] Further studies are needed to

Downloaded from http://cardiovascres.oxfordjournals.org/ by guest on May 10, 2012

clarify the contribution of AT1R to depression-like behaviour and the interaction between AT1R and S1R.

A strong association with depression has been well known in both heart failure and hypertension. Therefore, the pressure overload model, a mimic of hypertensive heart disease, was used as the experimental heart disease model in the present study. Other experimental heart failure models, such as that induced by myocardial ischaemia, have also been used widely. Recently, patients with coronary disease who screened as positive on depression screening test had a greater risk for adverse cardiovascular outcomes.[40] Therefore, the experimental heart failure model induced by myocardial ischaemia should also be used to test our hypothesis in the future.

4.6 Conclusion

In conclusion, these findings indicate that brain S1R expression was decreased in AB-H, and that this reduction in brain S1R expression contributed to both the exacerbation of cardiac dysfunction via enhanced sympathetic activity and the worsening of depression.

Acknowledgements

We express our sincere thanks to Naomi Shirouzu for help with the western blot analysis.

Conflict of interest: none declared.

Funding

This work was supported by Grants-in-Aid for Scientific Research from the Japan Society for the Promotion of Science (19890148, 23220013), Kaibara Morikazu Medical Science Promotion Foundation, Kyushu University Interdisciplinary Programmes in Education and Projects in Research Development, and the Salt Science Research Foundation (1136).

References

1. Havranek EP, Ware MG, Lowes BD. Prevalence of depression in congestive heart failure. *Am J Cardiol* 1999;**84**:348–350.
2. Vaccarino V, Kasl SV, Abramson J, Krumholz HM. Depressive symptoms and risk of functional decline and death in patients with heart failure. *J Am Coll Cardiol* 2001;**38**: 199–205.
3. Jiang W, Alexander J, Christopher E, Kuchibhatla M, Gauiden LH, Cuffe MS *et al.* Relationship of depression to increased risk of mortality and rehospitalization in patients with congestive heart failure. *Arch Intern Med* 2001;**161**:1849–1856.
4. Jünger J, Schellberg D, Müller-Tasch T, Raupp G, Zugck C, Haunstetter A *et al.* Depression increasingly predicts mortality in the course of congestive heart failure. *Eur J Heart Fail* 2005;**7**:261–267.
5. Abramson J, Berger A, Krumholz HM, Vaccarino V. Depression and risk of heart failure among older persons with isolated systolic hypertension. *Arch Intern Med* 2001;**161**:1725–1730.
6. Gradman AH, Alfayoumi F. From left ventricular hypertrophy to congestive heart failure: manegement of hypertensive heart disease. *Progr Cardiovasc Dis* 2006;**48**: 326–341.
7. Barton DA, Dawood T, lambert EA, Esler MD, Haikerwal D, Brenchley C *et al.* Sympathetic activity in major depressive disorder: identifying those at increased cardiac risk? *J Hypertens* 2007;**25**:2117–2124.
8. Grippo AJ, Moffitt JA, Johnson AK. Evaluation of baroreceptor reflex function in the chronic mild stress rodent model of depression. *Psychosom Med* 2008;**70**:435–443.
9. Mark AL. Sympathetic dysregulation in heart failure: mechanisms and therapy. *Clin Cardiol* 1995;**18**:I3–I8.
10. Hirooka Y, Kishi T, Sakai K, Takeshita A, Sunagawa K. Imbalance of central nitric oxide and reactive oxygen species in the regulation of sympathetic activity and neural mechanisms of hypertension. *Am J Physiol* 2011;**300**:R818–R826.
11. Bermack JE, Debonnel G. The role of sigma receptors in depression. *J Pharmacol Sci* 2005;**97**:317–336.
12. Skuza G, Rogóż Z. Antidepressant-like effects of PRE-084, a selective σ1 receptor agonist, in Albino Swiss and C57BL/6J mice. *Pharmacol Res* 2009;**61**:1179–1183.
13. Monnet FP. Sigma-1 receptor as regulator of neuronal intracellular Ca^{2+}; clinical and therapeutic relevance. *Biol Cell* 2005;**97**:873–883.
14. Kurata K, Takebayashi M, Morinobu S, Yamawaki S. β-estradiol, dehydroepiandrosterone, and dehydroepiandrosterone sulfate protect against N-methyl-D-aspartate-induced neurotoxicity in rat hippocampal neurons by different mechanisms. *J Pharmacol Exp Ther* 2004;**311**:237–245.
15. Zhang XJ, Liu LL, Jiang SX, Zhong YM, Yang XL. Activation of the sigma receptor 1 suppresses NMDA responses in rat retinal ganglion cells. *Neuroscience* 2011;**19**:110–116.
16. Bhuiyan MS, Fukunaga K. Stimulation of sigma-1 receptor signaling by dehydroepiandrosterone ameliorates pressure overload-induced hypertrophy and dysfunction in ovariectomized rats. *Expert Opi Ther Targets* 2009;**13**:1253–1265.
17. Moriyama Y, Yasue H, Yoshimura M, Mizuno Y, Nishiyama K, Tsunoda R *et al.* The plasma levels of dehydroepiandrosterone sulfate are decreased in patients with chronic heart failure in proportion to the severity. *J Clin Endocrinol Metab* 2000;**85**:1834–1840.
18. Ito K, Hirooka Y, Sunagawa K. Acquisition of brain Na sensitivity contributes to salt-induced sympathoexcitation and cardiac dysfunction in mice with pressure overload. *Circ Res* 2009;**104**:1004–1011.
19. Tagashira H, Bhuiyan S, Shioda N, Hasegawa H, Kanai H, Fukunaga K. σ1-receptor stimulation with fluvoxamine ameliorates transverse aortic constriction-induced myocardial hypertrophy and dysfunction in mice. *Am J Physiol* 2010;**299**:H1535–H1545.
20. Ito K, Hirooka Y, Sunagawa K. Blockade of mineralocorticoid receptors improves salt-induced left-ventricular systolic dysfunction through attenuation of enhanced sympathetic drive in mice with pressure overload. *J Hypertens* 2010;**28**:1449–1458.
21. Su TP, Wu XZ, Cone EJ, Shunkla K, Gund TM, Dodge AL *et al.* Sigma compounds derived from phencyclidine: identification of PRE-084, a new, selective sigma ligand. *J Pharmacol Exp Ther* 1991;**259**:543–550.
22. Penas C, Pascual-Font A, Mancuso R, Fores J, Casas C, Navarro X. Sigma receptor agonist 2-(4-morpholinethyl)1 phenylcyclohexanecarboxylate (Pre084) increases GDNF and BiP expression and promotes neuroprotection after root avulsion injury. *J Neurotrauma* 2011;**28**:831–840.
23. Sabino V, Cottone P, Zhao Y, Iyer MR, Sterado L Jr, Sterado L *et al.* The sigma receptor antagonist BD-1063 decreases ethanol intake and reinforcement in animal models of excessive drinking. *Neuropsychopharmacology* 2009;**34**:1482–1493.
24. Ito K, Hirooka Y, Kimura Y, Sagara Y, Sunagawa K. Ovariectomy augments hypertension through rho-kinase activation in the brain stem in female spontaneously hypertensive rats. *Hypertension* 2006;**48**:651–657.
25. Baudrie V, Laude D, Elghozi JL. Optimal frequency ranges for extracting information on cardiovascular autonomic control from the blood pressure and pulse interval spectrograms in mice. *Am J Physiol* 2007;**292**:R904–R912.
26. Roh DH, Kim HW, Yoon SY, Seo HS, Kwon YB, Kim KW *et al.* Intrathecal injection of the σ1 receptor antagonist BD1047 blockes both mechanical allodynia and increases in spinal NR1 expression during the induction phase of rodent neuropathic pain. *Anesthesiology* 2008;**109**:879–889.
27. Livak KJ, Schmittgen TD. Analysis of relative gene expression data using real-time quantitative PCR and the 2(-Delta Delta C(T)) method. *Methods* 2001;**25**:402–408.
28. Steru L, Chermat R, Thierry B, Simon P. The tail suspension test: A new method for screening antidepressants in mice. *Psychopharmacology* 1985;**85**:367–370.
29. Kumar A, Garg R, Gaur V, Kumar P. Nitric oxide mechanism in protective effects of imipramine and venlafaxine against acute immobilization stress-induced behavioral and biochemical alteration in mice. *Neurosci Lett* 2009;**467**:72–75.
30. Stefanski R, Justinova Z, Hayashi T, Takebayashi M, Goldberg SR, Su TP. Sigma1 receptor upregulation after chronic methamphetamine self-administration in rats: a study with yoked controls. *Psychopharmacology* 2004;**175**:68–75.
31. Rudick RA, Zirretta DK, Herndon RM. Clearance of albumin from mouse subarachnoid space: a measure of CSF bulk flow. *J Neurosci Methods* 1982;**6**:253–259.
32. Ruscher K, Shamloo M, Rickhag M, Ladunga I, Soriano L, Gisselsson L *et al.* The sigma-1 receptor enhances brain plasticity and functional recovery after experimental stroke. *Brain* 2011;**134**:732–756.
33. Alonso G, Phan V, Guillemain I, Saunier M, Legrand A, Anoal M *et al.* Immunocytochemical localization of the sigma$_1$ receptor in the adult rat central nervous system. *Neuroscience* 2000;**97**:155–170.
34. Ransohoff RM, Cardona AE. The myeloid cells of the central nervous system parenchyma. *Nature* 2010;**468**:253–262.
35. Aaron AH, Yelenis H, Craig AC Jr, Javier C, Keith RP. Sigma receptors suppress multiple aspects of microglial activation. *Glia* 2009;**57**:744–754.
36. Zucker IH. Novel mechanisms of sympathetic regulation in chronic heart failure. *Hypertension* 2006;**48**:1005–1011.
37. Parker LN, Odell WD. Control of adrenal androgen secretion. *Endocr Rev* 1980;**1**: 392–410.
38. Jankowska EA, Drohomirecka A, Ponikowska B, Witkowska A, Lopuszanska M, Szklarska A *et al.* Deficiencies in circulation testosterone and dehydroepiandrosterone sulphate, and depression in men with systolic chronic heart failure. *Eur J Heart Fail* 2010;**12**:966–973.
39. Saavedra JM, Sanches-Lemus E, Benicky J. Blockade of brain angiotensin II AT1 receptors ameliorates stress, anxiety, brain inflammation and ischemia: therapeutic implications. *Psychoneuroendocrinology* 2011;**36**:1–18.
40. Elderon L, Smolderen KG, Na B, Whooley MA. Accuracy and prognostic value of American Heart Association-recommended depression screening in patients with coronary heart disease: Data from the Heart and Soul Study. *Circ Cardiovasc Qual Outcomes* 2011;**4**:533–540.

Downloaded from http://cardiovascres.oxfordjournals.org/ by guest on May 10, 2012

Adaptation of the respiratory controller contributes to the attenuation of exercise hyperpnea in endurance-trained athletes

Tadayoshi Miyamoto, Masashi Inagaki, Hiroshi Takaki, Toru Kawada, Toshiaki Shishido, Atsunori Kamiya & Masaru Sugimachi

European Journal of Applied Physiology

ISSN 1439-6319
Volume 112
Number 1

Eur J Appl Physiol (2012) 112:237-251
DOI 10.1007/s00421-011-1968-2

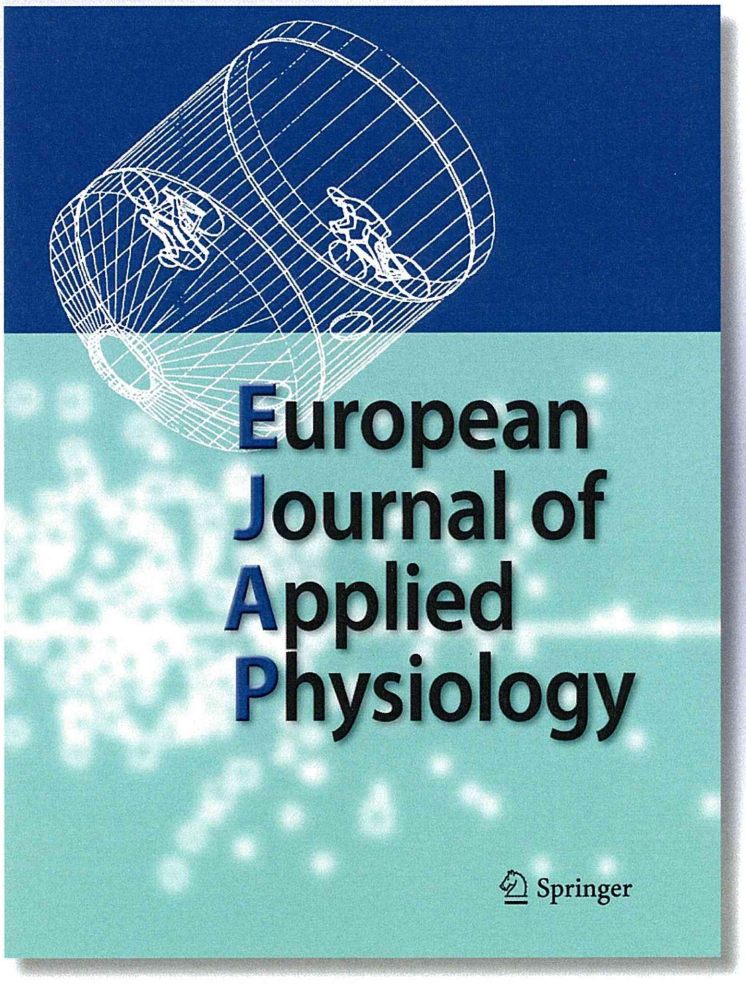

Springer

Your article is protected by copyright and all rights are held exclusively by Springer-Verlag. This e-offprint is for personal use only and shall not be self-archived in electronic repositories. If you wish to self-archive your work, please use the accepted author's version for posting to your own website or your institution's repository. You may further deposit the accepted author's version on a funder's repository at a funder's request, provided it is not made publicly available until 12 months after publication.

Author's personal copy

Eur J Appl Physiol (2012) 112:237–251
DOI 10.1007/s00421-011-1968-2

ORIGINAL ARTICLE

Adaptation of the respiratory controller contributes to the attenuation of exercise hyperpnea in endurance-trained athletes

Tadayoshi Miyamoto · Masashi Inagaki · Hiroshi Takaki · Toru Kawada · Toshiaki Shishido · Atsunori Kamiya · Masaru Sugimachi

Received: 8 December 2010 / Accepted: 9 April 2011 / Published online: 3 May 2011
© Springer-Verlag 2011

Abstract We have reported that minute ventilation [$\dot{V}_E$] and end-tidal CO_2 tension [P_{ETCO_2}] are determined by the interaction between central controller and peripheral plant properties. During exercise, the controller curve shifts upward with unchanged central chemoreflex threshold to compensate for the plant curve shift accompanying increased metabolism. This effectively stabilizes P_{ETCO_2} within the normal range at the expense of exercise hyperpnea. In the present study, we investigated how endurance-trained athletes reduce this exercise hyperpnea. Nine exercise-trained and seven untrained healthy males were studied. To characterize the controller, we induced hypercapnia by changing the inspiratory CO_2 fraction with a background of hyperoxia and measured the linear $P_{ETCO_2} - \dot{V}_E$ relation [$\dot{V}_E = S(P_{ETCO_2} - B)$]. To characterize the plant, we instructed the subjects to alter $\dot{V}_E$ voluntarily and measured the hyperbolic $\dot{V}_E - P_{ETCO_2}$ relation ($P_{ETCO_2} = A/\dot{V}_E + C$). We characterized these relations both at rest and during light exercise. Regular exercise training did not affect the characteristics of either controller or plant at rest. Exercise stimulus increased the controller gain (S) both in untrained and trained subjects. On the other hand, the P_{ETCO_2}-intercept (B) during exercise was greater in trained than in untrained subjects, indicating that exercise-induced upward shift of the controller property was less in trained than in untrained subjects. The results suggest that the additive exercise drive to breathe was less in trained subjects, without necessarily a change in central chemoreflex threshold. The hyperbolic plant property shifted rightward and upward during exercise as predicted by increased metabolism, with little difference between two groups. The $\dot{V}_E$ during exercise in trained subjects was 21% lower than that in untrained subjects ($P < 0.01$). These results indicate that an adaptation of the controller, but not that of plant, contributes to the attenuation of exercise hyperpnea at an iso-metabolic rate in trained subjects. However, whether training induces changes in neural drive originating from the central nervous system, afferents from the working limbs, or afferents from the heart, which is additive to the chemoreflex drive to breathe, cannot be determined from these results.

Keywords System analysis · Endurance training · Chemoreflex · Respiratory control · Exercise

Introduction

The respiratory chemoreflex is a negative feedback system that can be divided into two subsystems (Fig. 1a): a central ventilation controller (controlling element) and a peripheral plant (controlled element) (Defares 1964; Milhorn 1966; Berger et al. 1977; Kao 1963; Cunningham et al. 1986; Cummin and Saunders 1987; Khoo 2000). Recently, we have characterized these subsystems in an effectively open-loop condition and constructed a respiratory equilibrium diagram to illustrate the mechanisms of respiratory

Communicated by Susan A. Ward.

T. Miyamoto (✉)
Faculty of Health Sciences, Morinomiya University of Medical Sciences, 1-26-16 Nanko-Kita, Suminoe-Ku, Osaka City, Osaka 559-0034, Japan
e-mail: miyamoto@morinomiya-u.ac.jp

T. Miyamoto · M. Inagaki · H. Takaki · T. Kawada · T. Shishido · A. Kamiya · M. Sugimachi
Department of Cardiovascular Dynamics, National Cerebral and Cardiovascular Center Research Institute, Suita City, Osaka 565-8565, Japan

Author's personal copy

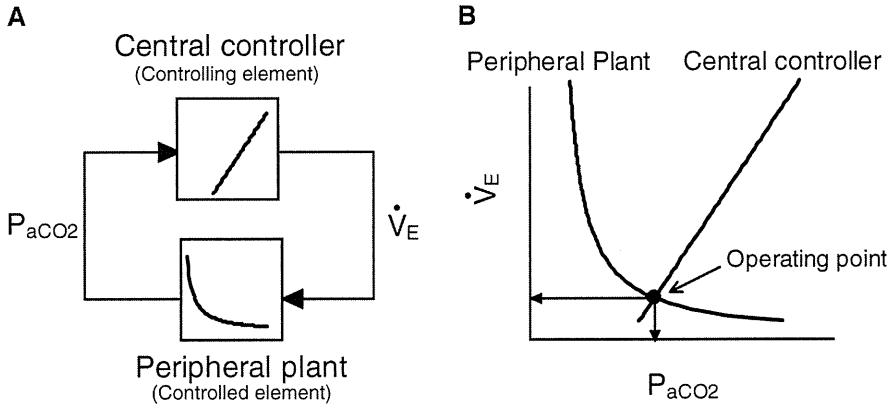

Fig. 1 Equilibrium diagram model of respiratory chemoreflex feedback system. **a** The respiratory chemoreflex system consists of two subsystems, the central controller and peripheral plant. **b** In the central controller the input parameter is arterial P_{CO_2} (P_{aCO_2}), the output parameter is minute ventilation ($\dot{V}_E$). The central controller can be characterized by observing changes in $\dot{V}_E$ in response to changes in P_{aCO_2}. In the peripheral plant, input is $\dot{V}_E$, and output is P_{aCO_2}. The peripheral plant can be characterized by observing changes in P_{aCO_2} in response to changes in $\dot{V}_E$. Since both relationships share common variables, the resultant operating point of ventilatory response under the closed-loop condition is determined by the intersection of the two relations

regulation at rest (Miyamoto et al. 2004) and during exercise (Ogoh et al. 2008) in humans. Briefly, the controller property approximates a straight line where minute ventilation ($\dot{V}_E$) increases as a function of arterial CO_2 tension (P_{aCO_2}). The plant property approximates a hyperbola with a positive asymptote where P_{aCO_2} decreases asymptotically as a function of $\dot{V}_E$. Respiration is determined from the intersection point (operating $\dot{V}_E$ and P_{aCO_2}) of these two curves in the respiratory equilibrium diagram (Fig. 1b). Several decades ago, Lloyd and Cunningham (1963) and Cummin and Saunders (1987) already proposed a model of chemoreflex control of breathing, which has come to be known as the "Oxford model". Furthermore, Cummin and Saunders (1987) have explained exercise hyperpnea using their conceptual frameworks to integrally characterize the regulation of human respiration.

The concept of an exercise drive to breathe that is additive to the chemoreflex drive to breathe (Casey et al. 1987; Duffin and McAvoy 1988; Duffin 1994) is now considered a common understanding. Although the use of respiratory equilibrium diagram has been described by Mahamed et al. (2001), there is no report of experimental study in humans that quantitatively validates the major mechanism of exercise hyperpnea based on integration of the controller and plant properties in the respiratory equilibrium diagram.

Regular exercise training induces a number of beneficial physiological changes in exercising muscles as well as cardiovascular and respiratory systems. Numerous reports have consistently shown that exercise training reduces $\dot{V}_E$ for any given level of work or O_2 uptake ($\dot{V}_{O_2}$) and lowers ventilatory equivalent ($\dot{V}_E/\dot{V}_{O_2}$) during submaximal load (Byrne-Quinn et al. 1971; Taylor and Jones 1979; Martin et al. 1979; Yerg et al. 1985; Casaburi et al. 1987b). However, none of these reports demonstrated quantitatively the relationship between reduced ventilatory requirement during exercise in trained subjects and ventilatory regulation by the respiratory chemoreflex system, and the association between reduced $\dot{V}_E$ and training-induced changes in controller and plant properties.

With respect to the controller properties, although previous studies indicated unchanged (Byrne-Quinn et al. 1971; Yerg et al. 1985; McConnell and Semple, 1996) or reduced (Miyamura et al. 1976) controller gain during exercise in trained subjects compared with untrained subjects, other controller parameters such as the operating point and central chemoreflex threshold to P_{CO_2} (P_{ETCO_2}-intercept) were not documented. Moreover, the change in plant property during exercise has not been estimated in trained or untrained subjects. The information provided by the operating point and P_{ETCO_2}-intercept would become much more meaningful when the controller and plant properties are integrated in the respiratory equilibrium diagram. In fact, McConnell and Semple (1996) and Caillaud et al. (1993) reported that endurance athletes showed the greatest rise in P_{ETCO_2} from rest to exercise. Taylor and Jones (1979) and Casaburi et al. (1987b) also reported that exercise training increased P_{ETCO_2} and reduced $\dot{V}_E$ for a given level of work or $\dot{V}_{O_2}$. Based on the fact that the operating points ($\dot{V}_E$ and P_{aco_2}) is determined by the integration of controller and plant properties in the respiratory equilibrium diagram, we hypothesized that the differences in the $\dot{V}_E$ response between trained and untrained subjects should be a result of the group

Author's personal copy

difference in exercise-induced changes in controller and/or plant properties.

In the present study, we compared exercise-induced changes in controller and plant properties in the respiratory equilibrium diagram between untrained and trained subjects. Quantitative analysis of two arcs provides us with a framework by which we can analytically evaluate how the unique value of $\dot{V}_E$ is determined by the respiratory chemoreflex system, how changes in the controller properties affect $\dot{V}_E$, and how changes in the plant properties affect $\dot{V}_E$. A constant work rate corresponding to the same $\dot{V}_{O_2}$ level was set individually to exclude intergroup difference in exercise metabolic demand. If metabolic demand during exercise is not matched across all subjects, it is difficult to detect only intergroup difference in the exercise-induced shift of plant property, a prime determinant of operating equilibrium point, in trained subjects.

The results of the present study indicate that an adaptation of the respiratory controller, but not that of plant, contributes to the attenuation of exercise hyperpnea at an iso-metabolic rate in trained subjects. In addition, the exercise-induced upward shift of the controller property is less in endurance-trained than in untrained subjects, indicating that the additive exercise drive to breathe is less in trained subjects, without necessarily a change in central chemoreflex threshold.

Methods

Nine trained and seven untrained healthy young male nonsmokers with no history or evidence of cardiac or pulmonary disease, whose ages ranged between 19 and 24 years [mean (SD): 21.3 (1.2) for trained and 19.7 (1.1) for untrained] were investigated. Subjects in the trained group were cycling athletes who had participated regularly in endurance exercise programs for several years. Subjects in the untrained group had a sedentary lifestyle. There were no differences in weight and height between the trained and untrained groups [172.9 (5.6) vs. 170.3 (6.3) cm; 62.0 (5.9) vs. 62.3 (7.4) kg]. All subjects gave written informed consent to participate in the present study after possible risks of participation were explained. The experimental protocol and consent form were reviewed and approved by the Human Subjects Committee of National Cerebral Cardiovascular Center and Morinomiya University of Medical Sciences.

Experimental apparatus and measurements

Ventilatory responses were measured using an open-circuit apparatus. The subjects breathed through a face mask attached to a low-resistance one-way valve with a built-in hot wire. The valve mechanism allowed subjects to inspire room air or a selected gas mixture from a 200-l plastic bag containing 0.0, 3.5, 5.0 or 6.0% CO_2 in 80% O_2 with N_2 balance. The total instrumental dead space was 200 ml.

Physiological data during the experiments were recorded by an automatic breath-by-breath respiratory gas analyzing system (AE-280S, Minato Medical Science Co., Osaka, Japan) consisting of a flow meter for the hot wire in the face mask, an O_2 analyzer made from a zirconium element, and an infrared CO_2 analyzer. We digitized expired flow, CO_2 and O_2 concentrations at 200 Hz, and derived tidal volume (V_T), respiratory rate (RR), $\dot{V}_E$, end-tidal CO_2 tension (P_{ETCO_2}), and end-tidal O_2 tension, $\dot{V}_{O_2}$, and CO_2 output ($\dot{V}_{CO_2}$) from the digitized data. We took into account the time delay during gas concentration measurements in these calculations. We used P_{ETCO_2} as a surrogate for P_{aCO_2}. Venous blood lactate and potassium (K^+) concentration were measured using a blood gas analyzer (IL 1620, Instrumentation Laboratory Co., Barcelona, Spain).

Experimental protocols

Maximal exercise test

On the first day, each subject performed maximal cycle exercise to compare maximal aerobic capacity and exercise ventilatory response between the two groups. An incremental protocol on a computer-controlled bicycle ergometer (232CXL, Combi Co., Tokyo) was used to assess maximal oxygen uptake ($\dot{V}_{O_{2max}}$) and ventilatory threshold by the V-slope method (Beaver et al. 1986). The work rate was set initially at 20 W and increased by 20 W every minute until the subject could no longer maintain the pedaling frequency of 60 rpm despite strong verbal encouragement.

Assessment of respiratory equilibrium diagram

On the experimental day, a hypercapnia test and a hyper/hypoventilation test were performed sequentially to characterize the controller and plant properties, respectively, for the construction of respiratory equilibrium diagrams. An at-rest protocol and an exercise protocol were performed on different days. Regarding the exercise level, the subjects cranked a bicycle ergometer at a constant predetermined work rate corresponding to a $\dot{V}_{O_2}$ level of 0.80 l/min throughout each test.

The subjects were instructed to avoid strenuous exercise and food with a high salt content for 24 h before the tests, and were also required to abstain from consuming food,

Author's personal copy

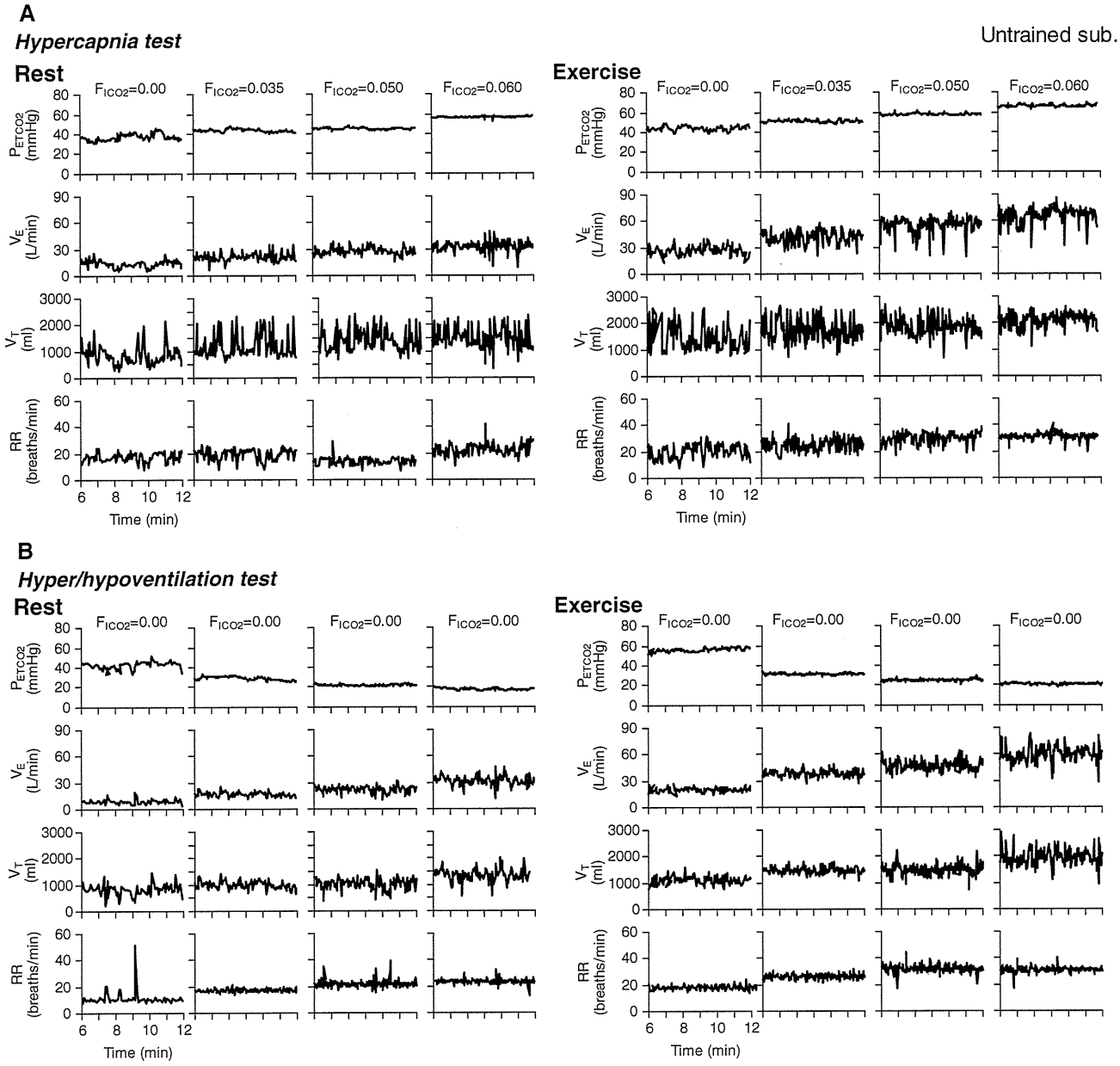

Fig. 2 A representative example of breath-by-breath time courses of P_{ETCO_2}, $\dot{V}_E$, V_T and RR at rest and during exercise in an untrained subject during open–loop respiratory chemoreflex control of $\dot{V}_E$ and P_{ETCO_2} in hypercapnia test (**a**) and hyper/hypoventilation test (**b**). Accompanying increases in F_{ICO_2} from 0 to 0.06, P_{ETCO_2}, $\dot{V}_E$, V_T and RR increase both at rest and during exercise. P_{ETCO_2} and $\dot{V}_E$ at rest and during exercise reach steady-states in 8–10 min

alcohol or caffeine for 3 h preceding the tests. The subjects remained in a fasting state throughout the two tests that lasted approximately 4 h. Before testing, an intravenous catheter (0.47 mm ID, 24 gauge) for blood collection was placed in the forearm of the subject seated in a comfortable chair. Venous blood samples (2.5 ml) were collected at 11 min of each 12-min trial described below.

Hypercapnia test Each hypercapnia test consisted of four trials each under resting and exercising conditions (Figs. 2a, 3a). Hypercapnia was induced by changing the level of inspired CO_2 concentrations (F_{ICO_2} = 0.0, 0.035, 0.05 or 0.06, F_{IO_2} = 0.80 with N_2 balance). The subject breathed each gas mixture for 12 min and then breathed room air during the interposing interval of approximately 10–15 min (Miyamoto et al. 2004). The 12-min duration was long enough to permit carbon dioxide tension to reach its new steady-state value at the central chemoreceptors (Lloyd and Cunningham 1963; Honda et al. 1983; Poon and Greene 1985; Cummin and Saunders 1987). The order

Author's personal copy

of the hypercapnia trials was randomized in each subject. All trials were performed under hyperoxic condition to suppress O_2-sensitive chemoreflexes (Lloyd and Cunningham 1963; Ohyabu et al. 1982; Robbins 1988; Mohan and Duffin 1997).

Hyper/hypoventilation test Each hyper/hypoventilation test consisted of four trials each under resting and exercising conditions (Figs. 2b, 3b). Subjects were instructed to breathe at different respiratory rates and tidal volumes to match a visual display of ventilation curves on a screen monitor (Miyamoto et al. 2004). For three levels of hyperventilation, the subjects breathed according to ventilation curves at respiratory rates and tidal volumes mimicking those recorded during the hypercapnia trials (F_{ICO_2} = 0.035, 0.05 or 0.06). For one level of hypoventilation, the subjects were asked to breathe following a breathing curve at 92% respiratory rate and 88% tidal volume measured when F_{ICO_2} was 0.0%. Each trial lasted 12 min with interposing intervals. All trials were started after $\dot{V}_E$ and P_{ETCO_2} values recovered to the resting levels. All trials were performed under hyperoxic condition ($F_{ICO_2} = 0.80$, $F_{IO_2} = 0.0$ with N_2 balance).

Data analysis

Because preliminary measurements indicated that both $\dot{V}_E$ and P_{ETCO_2} reached steady states in the last 2 min of each trial, the steady-state $\dot{V}_E$ and P_{ETCO_2} were obtained by averaging the respective data for the last 2 min. To characterize the controller property, we performed linear regression of $\dot{V}_E$ against P_{ETCO_2} [$\dot{V}_E = S(P_{ETCO_2} - B)$]; where S is the slope, and B is the P_{ETCO_2}-intercept (Lloyd and Cunningham 1963; Cummin and Saunders 1987). To characterize the plant property, we fitted a metabolic hyperbola ($P_{ETCO_2} = A/\dot{V}_E + C$) modified from the original metabolic hyperbola (Cunningham et al. 1986; Whipp and Pardy 1986) to the measured data (see Appendix). Hereafter in this paper, we refer to our metabolic hyperbola as the modified metabolic hyperbola. The measured operating point for each subject was defined to be the steady-state values of $\dot{V}_E$ and P_{ETCO_2} obtained during the F_{ICO_2} = 0.00 trial without visual feedback (i.e., during spontaneous breathing).

Statistical analysis

All values are presented as mean (SD). Statistical significance was accepted at $P < 0.05$. Two way analysis of variance (ANOVA) was performed with exercise stimulus as one factor (i.e., the difference between rest and exercise conditions) and exercise training as the other factor (i.e., the difference between untrained and trained subjects). When the interaction effect was statistically significant ($P < 0.05$), post-hoc analysis using Tukey test was performed for pair-wise comparisons (Glantz and Slinker 2001).

Results

The trained group had higher maximal oxygen uptake ($\dot{V}_{O_{2max}}$) [3.6 (0.3) vs. 2.7 (0.1) l/min, $P < 0.01$], higher $\dot{V}_{O_{2max}}$ per kg body weight [59.1(6.7) vs. 44.6 (6.9) ml/min/kg, $P < 0.01$] and higher ventilatory threshold [2.5 (0.5) vs. 1.4 (0.3) l/min, $P < 0.01$] compared to the untrained group. The trained group had the slightly higher value of P_{ETCO_2} at $\dot{V}_{O_{2max}}$ [39.3 (2.4) vs. 36.3 (4.8) mmHg], but was not significantly different between two groups. The maximal minute ventilation ($\dot{V}_{Emax}$) was also higher in the trained than in the untrained group [148.9 (12.9) vs. 121.5 (22.0) l/min, $P < 0.01$]. The higher $\dot{V}_E$ was due to larger V_T, because RR was not significantly different between two groups.

Table 1 summarizes the gas-exchange variables at rest and during exercise under spontaneous breathing ($F_{ICO_2} = 0.0$). Exercise stimulus significantly increased all the gas-exchange variables in both untrained and trained groups. The significant interaction effect observed for $\dot{V}_E$ indicated that the exercise-induced $\dot{V}_E$ increase was smaller in the trained than in the untrained group. Although the exercise stimulus significantly increased plasma potassium level, it did not significantly affect lactate level. There were no significant differences in plasma potassium and lactate levels between the untrained and trained groups.

Panel A of Figs. 2 and 3 show representative examples of breath-by-breath time courses of P_{ETCO_2}, $\dot{V}_E$, V_T and RR under various F_{ICO_2} at rest and during exercise in an untrained and a trained subject, respectively. When F_{ICO_2} increased from 0 to 0.06, P_{ETCO_2}, $\dot{V}_E$, V_T and RR increased in both trained and untrained subjects. Both P_{ETCO_2} and $\dot{V}_E$ at rest and during exercise reached steady states in 8–10 min.

Panel B of Figs. 2 and 3 illustrate the effects of changes in $\dot{V}_E$ on P_{ETCO_2} at rest and during exercise in an untrained and a trained subject, respectively. Hypoventilation increased P_{ETCO_2} while hyperventilation decreased P_{ETCO_2}. P_{ETCO_2} reached steady states in 8–10 min at rest and during exercise in both untrained and trained subjects.

Figure 4 shows the characteristics of controller (A) and plant (C) (left panels) at rest and during exercise obtained from the same untrained subject shown in Fig. 2, and the controller (B) and plant (D) characteristics (right panels)

Author's personal copy

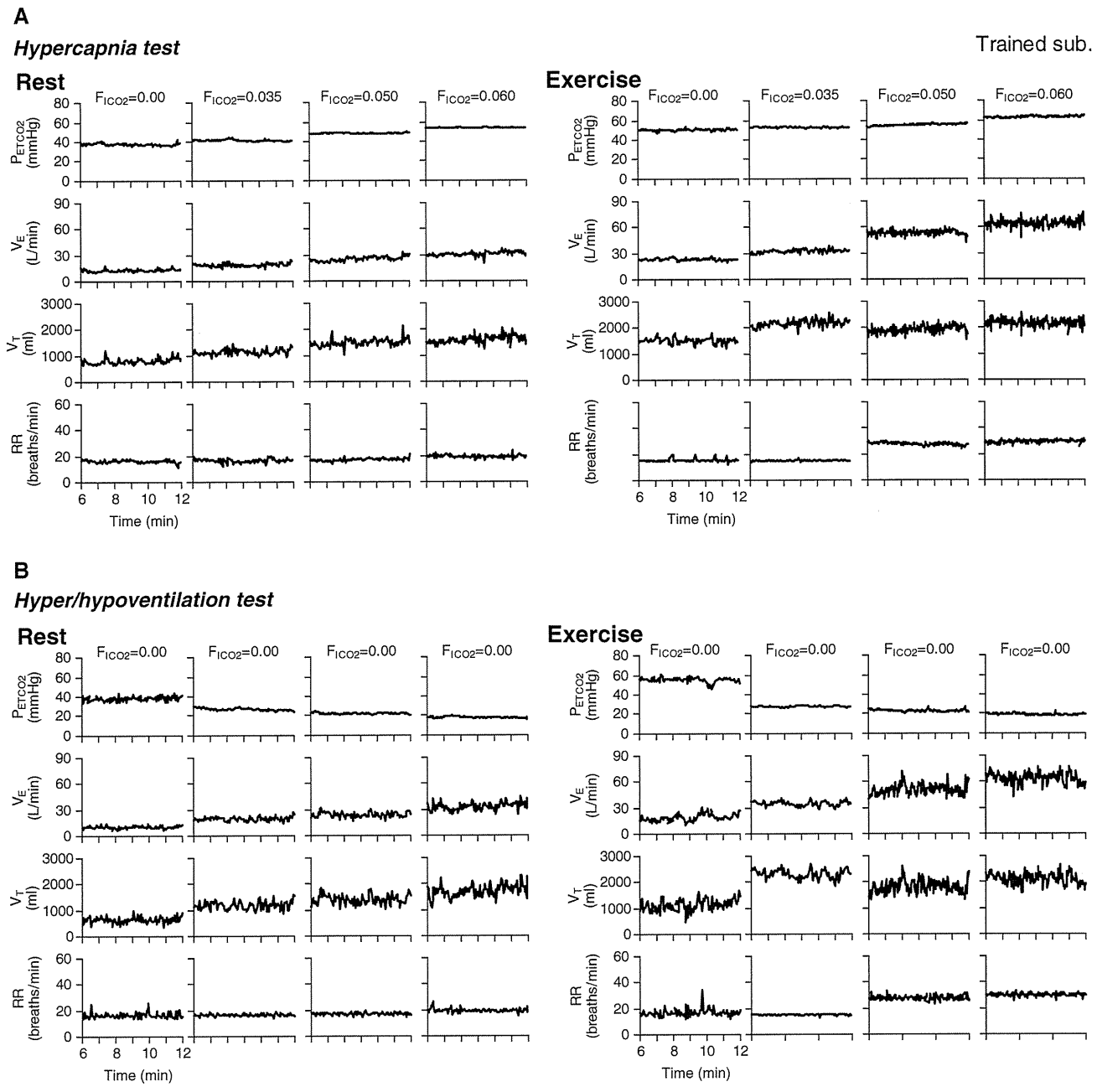

Fig. 3 A representative example of breath-by-breath time courses of P_{ETCO_2}, $\dot{V}_E$, V_T and RR at rest and during exercise in a trained subject during open-loop respiratory chemoreflex control of $\dot{V}_E$ and P_{ETCO_2} in hypercapnia test (**a**) and hyper/hypoventilation test (**b**). Hypoventilation increases P_{ETCO_2} while hyperventilation decreases P_{ETCO_2}. P_{ETCO_2} reaches steady states in 8–10 min at rest and during exercise

obtained from the same trained subject shown in Fig. 3. $\dot{V}_E$ increased linearly with increase in P_{ETCO_2} at rest and during exercise, both in representative trained and untrained subjects (Fig. 4a, b) and in pooled data ($r^2 = 0.808$–0.995 in all subjects; Fig. 5). The slope of the regression line, or the controller gain, was significantly increased by the exercise stimulus but was not different between the untrained and trained groups (Table 2). Significant interaction and main effects were observed for the P_{ETCO_2}-intercept (B). A post-hoc analysis revealed that the P_{ETCO_2}-intercept (B) during exercise was greater in the trained than in the untrained group (Table 2).

The effects of voluntary $\dot{V}_E$ changes on P_{ETCO_2} at rest and during exercise are shown in Figs. 4c and d, 6. The plant property approximated the modified metabolic hyperbola reasonably in both untrained and trained groups ($r^2 = 0.962$–0.996 in all subjects). The horizontal lines indicate the asymptotes of the modified hyperbolas. The

Author's personal copy

Table 1 Effects of regular exercise training on the response of gas-exchange variables from rest to exercise during the spontaneous breathing (0% F_{ICO_2} trial)

	Untrained (UT) ($n = 7$)		Trained (Tr) ($n = 9$)		ANOVA (P value)		
					Main effect		Interaction effect
	Rest (R)	Exercise (Ex)	Rest (R)	Exercise (Ex)	UT vs. Tr	R vs. E	UT vs. Tr × R vs. Ex
$\dot{V}_E$ (L/min)	10.6 ± 1.5	31.2 ± 4.0	12.1 ± 2.0	24.6 ± 2.7**	0.015	<0.001	<0.001
P_{ETCO_2} (mmHg)	38.7 ± 2.1	45.0 ± 4.9	39.3 ± 3.6	49.1 ± 3.3	ns	<0.001	ns
VT (mL)	702 ± 126	1351 ± 404	770 ± 155	1300 ± 230	ns	<0.001	ns
RR (breaths/min)	16.2 ± 4.6	25.0 ± 5.8	16.6 ± 4.7	20.2 ± 3.7	ns	0.004	ns
$\dot{V}_{O_2}$ (mL/min)	249 ± 79	836 ± 43	258 ± 23	842 ± 60	ns	<0.001	ns
$\dot{V}_{CO_2}$ (mL/min)	181 ± 18	762 ± 80	219 ± 21	734 ± 63	ns	<0.001	ns
K^+ (mmol/L)	4.1 ± 0.2	4.3 ± 0.2	4.0 ± 0.2	4.3 ± 0.1	ns	<0.001	ns
LA^- (mmol/L)	1.3 ± 0.4	1.3 ± 0.4	1.2 ± 0.6	1.0 ± 0.4	ns	ns	ns

Values are mean ± SD

$\dot{V}_E$, minute ventilation; P_{ETCO_2}, end-tidal pressures for CO_2; V_T, tidal volume; RR, respiratory rate; $\dot{V}_{O_2}$, oxygen uptake; $\dot{V}_{CO_2}$, carbon dioxide output; LA^-, blood lactic acid concentration; K^+, plasma potassium concentration

** $P < 0.01$ vs. UT during exercise

modified metabolic hyperbola shifted rightward and upward during exercise as predicted by an increased metabolism. The exercise stimulus increased the numerator A of the modified metabolic hyperbola but decreased the asymptote parameter C in both groups (Table 2).

Exercise stimulus increased the controller gain (S) by more than 50% in both groups. In contrast, exercise stimulus decreased the plant gain (G_P) calculated by the reciprocal of the slope of the modified metabolic hyperbola at the operating point, in both groups (Table 2). The significant interaction effect suggests that the absolute value in G_P during exercise was smaller in the untrained than in the trained group. During exercise, the estimated total loop gain at the operating point, i.e., product of the controller gain and plant gain, was significantly higher in the trained than in the untrained group.

The respiratory equilibrium diagram was constructed by plotting the controller and plant properties together on the same graph (Figs. 4e and f, 7). The intersection point between the controller and plant curves predicts the closed-loop operating point of respiration. Exercise stimulus moved the operating point rightward and upward in both groups, indicating that the exercise stimulus increased both P_{ETCO_2} and $\dot{V}_E$. Furthermore, the increase in operating $\dot{V}_E$ during exercise was smaller and the increase in P_{ETCO_2} was greater in the trained group than that in the untrained group.

As shown in Fig. 8a and b, P_{ETCO_2} and $\dot{V}_E$ predicted from the intersection point on the respiratory equilibrium diagram conformed reasonably well to the values actually measured. The regression line for P_{ETCO_2} was $y = 0.98x + 2.3$ ($r^2 = 0.921$, SEE = 1.1, $P < 0.001$). The regression line for $\dot{V}_E$ was $y = 0.97x + 0.80$ ($r^2 = 0.985$, SEE = 2.0, $P < 0.001$).

Discussion

To the best of our knowledge, this is the first report that quantitatively describes the mechanism of attenuated exercise hyperpnea in endurance-trained athletes by integrating the controller and plant properties in the respiratory equilibrium diagram. The present results show that the adaptation mechanism of central controller, but not that of peripheral plant, contributes to the attenuation of exercise hyperpnea at an iso-metabolic rate in trained subjects. In addition, the exercise-induced upward shift of the controller property is less in endurance-trained than in untrained subjects, indicating that the additive exercise drive to breathe is less in trained subjects without necessarily a change in central chemoreflex threshold.

Interpretation of the operating point of respiration using the respiratory equilibrium diagram

Our group has shown that the operating point of respiration at rest (Miyamoto et al. 2004) and during exercise (Ogoh et al. 2008) can be described by the point of intersection of the controller and plant curves in the respiratory equilibrium diagram. The concept of using the respiratory equilibrium diagram has been proposed by Mahamed et al. (2001). Indeed, operating P_{ETCO_2} and $\dot{V}_E$ predicted from the

Author's personal copy

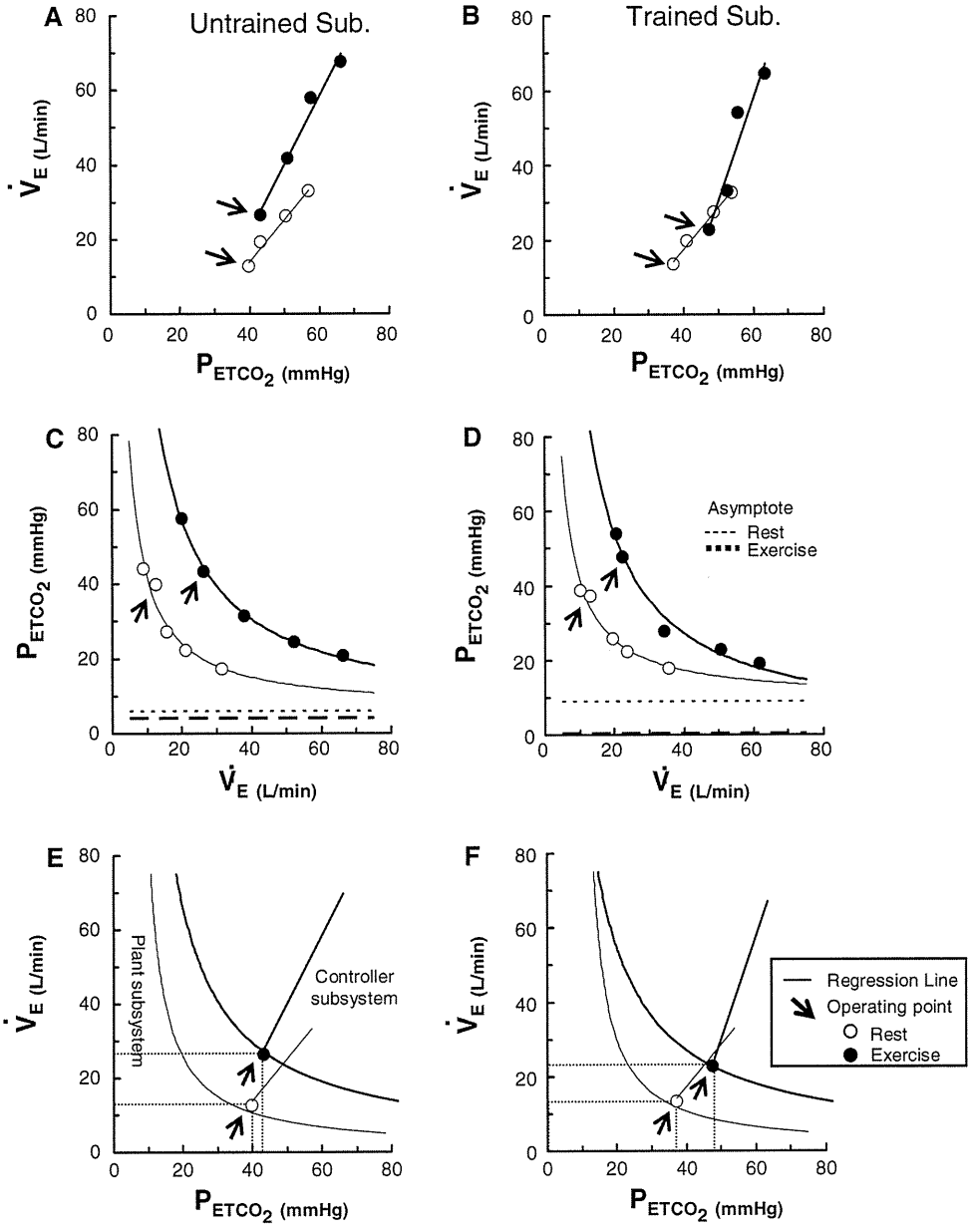

Fig. 4 Characteristics of central controller (**a**, **b**), peripheral plant (**c**, **d**) and equilibrium diagram (**e**, **f**) at rest and during exercise in representative untrained and trained subjects. **a** and **b** The central controller is characterized by a linear P_{ETCO_2}–$\dot{V}_E$ relation. $\dot{V}_E$ increases linearly with increase in P_{ETCO_2} during resting and exercising conditions in untrained (**a**) and trained (**b**) subjects. **c** and **d** The peripheral plant is characterized by a modified metabolic hyperbola. There is a good fit between measured data and the modified hyperbola in the two representative subjects. **e** and **f** The operating points estimated from the equilibrium diagram (intersection of central controller and peripheral plant plots) are very close to the measured values at rest (*open circles*) and during exercise (*closed circles*) in both representative cases

intersection point on the respiratory equilibrium diagram conformed reasonably well to the values actually measured regardless of rest, exercise, and/or physical conditions (Fig. 8). The present investigation extends previous studies by demonstrating the shifts of the operating points in the respiratory equilibrium diagram during exercise in untrained and trained subjects (Fig. 7).

Exercise stimulus moved the plant property right and upward (Fig. 6), reflecting increased metabolism. In the untrained group, if the exercise stimulus had not affected the controller property, the operating point during exercise would have been the intersecting point between the fine line and the bold hyperbola in Fig. 7a. In that case, P_{ETCO_2} would have increased to approximately 50 mmHg. However, the exercise stimulus moved the controller property toward higher $\dot{V}_E$ (Figs. 5, 7), which effectively stabilized P_{ETCO_2} within the normal range, at the expense of exercise hyperpnea.

In the trained group, because the intersection point between the fine line and bold hyperbola and that between the bold line and bold hyperbola is very close (Fig. 7b), the exercise-induced upward shift of the controller property did not contribute much to stabilize P_{ETCO_2}, thus attenuating exercise hyperpnea resulting in increased P_{ETCO_2} (Table 2). McConnell and Semple (1996) and Caillaud et al. (1993) reported that the endurance athletes showed the greatest rise in P_{aCO_2} or P_{ETCO_2} from rest to exercise. Taylor and Jones (1979) and Casaburi et al. (1987b) also

Author's personal copy

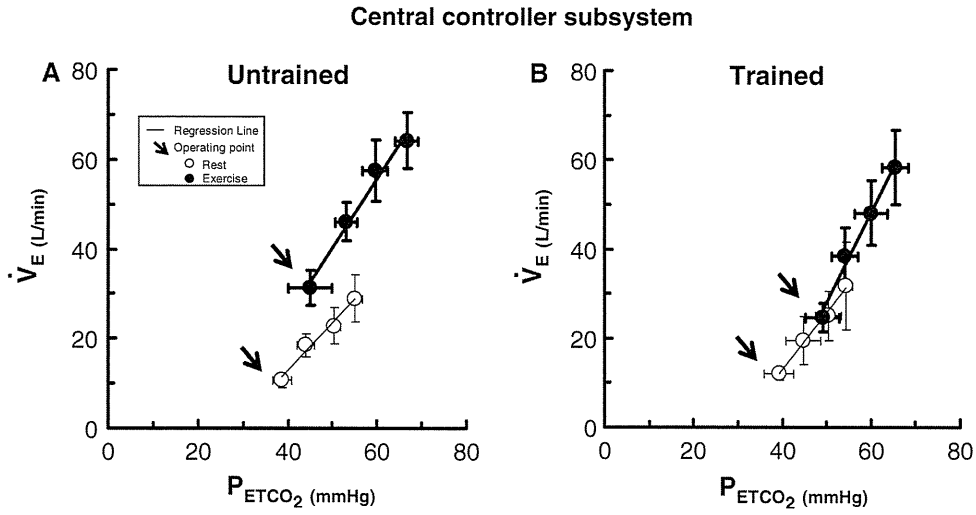

Fig. 5 Characteristics of central controller subsystem at rest and during exercise obtained from pooled data of all untrained and trained subjects. $\dot{V}_E$ increases linearly with P_{ETCO_2} during resting and exercising conditions in both groups ($r^2 = 0.808$–0.995 in all subjects). The slope of the regression line for pooled data, which represents the gain of the controller, is increased by exercise in both groups. On the other hand, exercise decreases the intercept (B) in untrained, but increases B in trained subjects. **a** (untrained): The averaged regression line is $\dot{V}_E = 1.1\,(P_{ETCO_2} - 27.3)$ at rest and $\dot{V}_E = 1.5\,(P_{ETCO_2} - 21.3)$ during exercise. **b** (trained): The averaged regression line is $\dot{V}_E = 1.2\,(P_{ETCO_2} - 27.3)$ at rest and $\dot{V}_E = 2.0 \times (P_{ETCO_2} - 34.2)$ during exercise. *Arrows* denote operating points. *Horizontal* and *vertical bars* indicate ±SD

Table 2 Effects of regular exercise training on changes in central controller and peripheral plant properties, and respiratory total loop gain from rest to exercise

	Untrained (UT)		Trained (Tr)		ANOVA (P value)		
	($n = 7$)		($n = 9$)		Main effect		Interaction effect
	Rest (R)	Exercise (Ex)	Rest (R)	Exercise (Ex)	UT vs. Tr R vs. E		UT vs. Tr × R vs. Ex
Central controller							
S (mL min^{-1} mmHg^{-1})	1.1 ± 0.3	1.5 ± 0.5	1.2 ± 0.4	2.0 ± 0.5	ns	<0.001	ns
B (mmHg)	26.6 ± 5.5	21.3 ± 11.1	27.3 ± 7.3	34.2 ± 5.3*	0.039	ns	0.018
Peripheral plant							
A (mL min mmHg)	305 ± 76	1170 ± 201	344 ± 84	1154 ± 193	ns	<0.001	ns
C (mL min^{-1})	8.5 ± 4.2	5.3 ± 4.4	7.6 ± 2.2	1.5 ± 3.4	ns	0.004	ns
Gp (mL min^{-1} mmHg)	−2.7 ± 0.7	−1.2 ± 0.3	−2.4 ± 0.6	−1.9 ± 0.3*	ns	<0.001	0.018
Total loop gain	2.8 ± 0.7	2.0 ± 1.0	3.0 ± 1.4	3.7 ± 1.1**	0.041	ns	0.047

Values are mean ± SD

Central controller, $\dot{V}_E = S(P_{ETCO_2} - B)$; S, central controller gain; B, P_{ETCO_2}-intercept; Peripheral plant, $P_{ETCO_2} = A/\dot{V}_E + C$; G_P, peripheral plant gain at operating point

** $P < 0.01$ and * $P < 0.05$ vs. UT during exercise

showed that exercise training increased P_{aCO_2} and reduced $\dot{V}_E$ for any given level of work or $\dot{V}_{O_2}$. These observations are consistent with our findings. The significance of training-induced change in controller property during exercise, resulting in decreased $\dot{V}_E$ may be in augmenting the total loop gain of the respiratory chemoreflex (Table 2), rather than in stabilizing $\dot{V}_{O_2}$, as discussed in the next paragraphs.

Interpretation of the total loop gain of respiratory control using the respiratory equilibrium diagram

Respiratory homeostasis is maintained by a powerful feedback control system mediated by P_{aCO_2} (Defares 1964; Milhorn 1966; Cunningham et al. 1986; Duffin et al. 2000). The magnitude of this control capability can be expressed as the "total loop gain" (Berger et al. 1977;

Author's personal copy

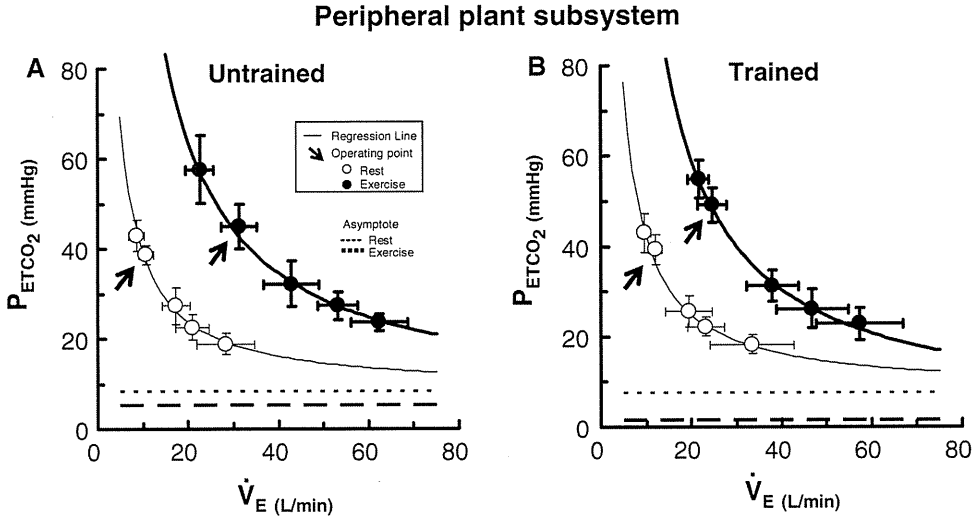

Fig. 6 Characteristics of peripheral plant subsystem at rest and during exercise obtained from pooled data of all untrained and trained subjects. The $\dot{V}_E - P_{ETCO_2}$ relationship approximates the modified metabolic hyperbola reasonably well both at rest and during exercise in both groups ($r^2 = 0.962$–0.996 in all subjects). The hyperbolic plant property shifts rightward and upward during exercise as predicted by increased metabolism. The mean value of the numerator A of the parabola increases from rest to exercise, while the asymptote constant C decreases in both groups. There is little difference between two groups in the exercise-induced shift, although the asymptote constant C tends to be lower in trained subjects than in untrained subjects. **a** (untrained): The averaged fitted hyperbola is $P_{ETCO_2} = 305/\dot{V}_E + 8.5$ at rest and $P_{ETCO_2} = 1,170/\dot{V}_E + 5.3$ during exercise. **b** (trained): The averaged fitted hyperbola is $P_{ETCO_2} = 344/\dot{V}_E + 7.6$ at rest and $P_{ETCO_2} = 1,154/\dot{V}_E + 1.5$ during exercise. *Arrows* denote operating points. *Horizontal* and *vertical bars* indicate ±SD

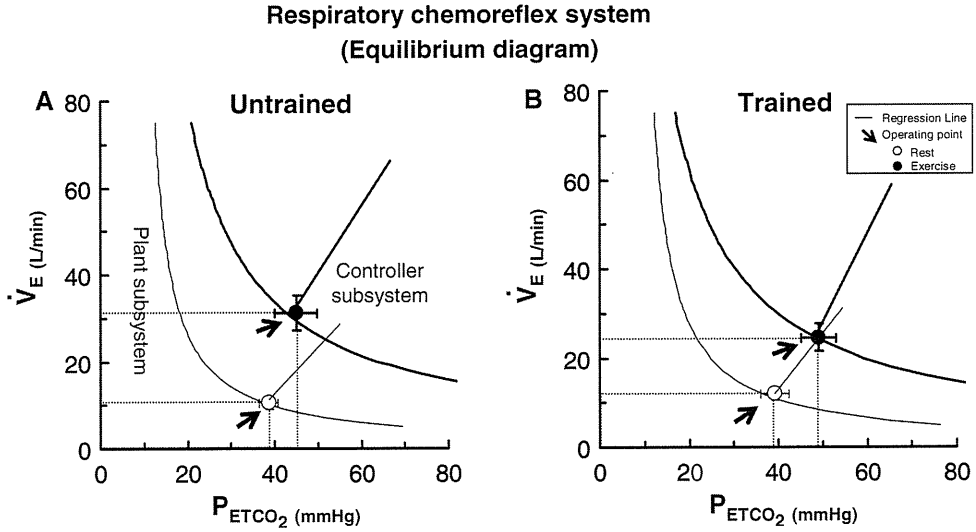

Fig. 7 Equilibrium diagrams at rest and during exercise in untrained and trained subjects. The operating points of chemoreflex system estimated as the intersection between the controller and plant curves are very close to those measured during closed-loop spontaneous breathing at rest (*open circles*) and during exercise (*closed circles*) in untrained (**a**) and trained (**b**) groups. In untrained group (**a**), exercise shifts the operating point by shifting the controller curve to the direction of decreased P_{ETCO_2}, which compensates for the shift of the plant curve accompanying increased metabolism. Compared with untrained group, strenuous regular exercise training almost abolishes the exercise-induced upward shift of the controller, but not the plant curve, thus attenuates exercise hyperpnea

Honda et al. 1983; Khoo 2000). In the respiratory equilibrium diagram, the total loop gain of respiratory control is calculated from the product of controller gain and plant gain at the intersection point. In the present study, the total loop gain was not different between the untrained and trained subjects at rest, but was significantly higher in the trained than in the untrained subjects during exercise (Table 2).

Author's personal copy

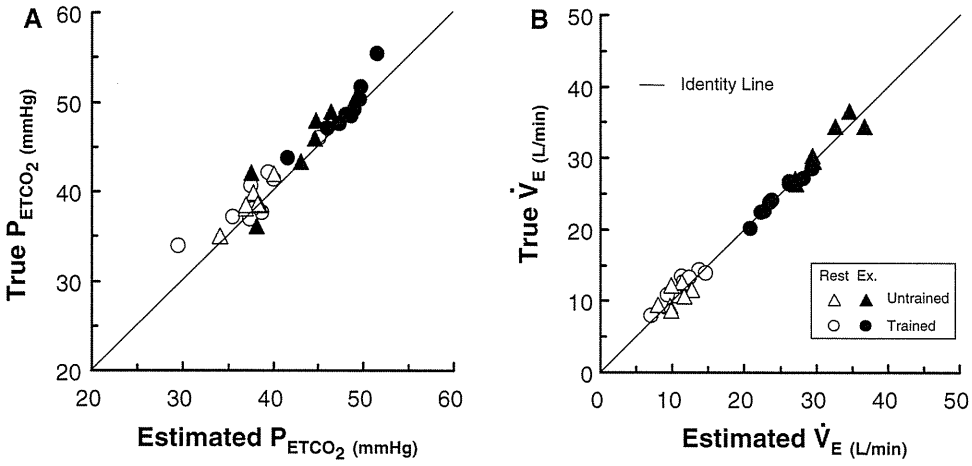

Fig. 8 Correlation between operating points estimated by the equilibrium diagram and those measured. **a** The estimated P_{ETCO_2} correlate closely with measured P_{ETCO_2} ($y = 0.98x + 2.3$, $r^2 = 0.927$, SEE = 1.1, $P < 0.001$). The *solid line* indicates the line of identity. **b** The estimated $\dot{V}_E$ also correlate closely with measured $\dot{V}_E$ ($y = 0.97x + 0.80$, $r^2 = 0.985$, SEE = 2.0, $P < 0.001$). The *solid line* indicates the line of identity. *Open and closed symbols* indicate rest and exercise conditions, respectively. *Triangles* and *circles* indicate untrained and trained subjects, respectively

Based on the modified metabolic hyperbola, plant gain decreases markedly as $\dot{V}_E$ increases (Fig. 6). Because $\dot{V}_E$ increases significantly during exercise, the plant gain would have been much smaller, if the exercise stimulus had not changed the plant property. The right and upward shift of the plant property during exercise contributed to increase the plant gain at higher $\dot{V}_E$ range. Despite the right and upward shift in the plant property, however, the plant gain at the operating point was significantly decreased during exercise in both the untrained and trained groups. The exercise-induced increase in controller gain may therefore be important to compensate for the decreased plant gain during exercise.

Although the total loop gain did not differ between the untrained and trained groups at rest, it was significantly higher in the trained than in the untrained group during exercise (Table 2). The increased total loop gain in the trained group is the result of an increase in plant gain because the equilibrium point is at a higher P_{CO_2}; and therefore is not related to adaptation in the chemoreflex control of CO_2.

Exercise-induced shift in the controller property

A large number of the physiologists accept the exercise-induced upward shift of the controller property, although the effect of exercise stimulus on the controller gain (CO_2 sensitivity) varies among studies. Casey et al. (1987) demonstrated that the central chemoreceptor threshold is unchanged by exercise, and supported the neuro-humoral theory of exercise ventilation. The concept of an exercise drive to breathe that is additive to the chemoreflex drive to breathe is now considered a common understanding. In the present study, the exercise stimulus increased the controller gain (S) both in untrained and trained subjects. However, the P_{ETCO_2}-intercept (B) during exercise was greater in the trained than in the untrained group, implying that exercise-induced upward shift of the controller property was less in the trained than in the untrained subjects (Table 2; Fig. 5). On the other hand, the P_{ETCO_2}-intercept (B) hardly shifted indicating that the chemoreflex threshold did not change. These findings thus suggest that the additive exercise drive to breathe is less in trained subjects, but not necessarily due to a change in central chemoreflex threshold.

A variety of mechanisms have been postulated to explain the exercise-induced upward shift of the controller property during exercise, leading to exercise hyperpnea (Eldridge and Waldrop 1991; Strange et al. 1993; Eldridge 1994; Mateika and Duffin 1995; Harms and Dempsey 1999), such as "irradiation" of signals from the motor cortex (Wood et al. 2003), stimulation of neural receptors in the exercising muscles (Kao 1963; McCloskey and Mitchell 1972; Smith et al. 2006; Amann et al. 2008), stimulation of chemoreceptors by humoral factors released from the exercising muscles (Casaburi et al. 1987b; Johnson et al. 1998), stimulation of chemoreceptors in the lungs by mixed venous P_{CO_2} (Wasserman et al. 1986), and thermoregulation (Hayashi et al. 2006). Furthermore, the recent experiments of Bell (2006) and Dempsey (2006) have shown that both peripheral afferent feedback and central command contribute. The fact that the effects of exercise stimulus on the controller property differ between untrained and trained subjects may contribute, in part, to the diverse results reported on the exercise-induced change in the controller property. The training-induced change in

Author's personal copy

controller property during exercise is probably independent of humoral mechanisms, because the exercise was performed at an intensity below the ventilatory threshold (Table 1). Sporer et al. (2007) showed that the entrainment of breathing rhythm to exercise rhythm may also be a factor affecting the exercise drive to breathe. However, it is unlikely that this mechanism is involved in the difference in controller property between two groups, because there were no intergroup differences in the breathing patterns at rest and during exercise. Consequently, other neural drives originating from the central nervous system, afferents from the working limbs or afferents from the heart, which is additive to the chemoreflex drive to breathe, may be involved in exercise-induced upward shift of the controller property, leading to exercise hyperpnea.

According to the results of Duffin (2005), a decrease in the central-chemoreflex threshold [P_{ETCO_2}-intercept (B)] can be explained by the effects of acute and/or chronic acid–base adjustments (e.g., reduced [strong ion difference]). In our study, it is unlikely that a difference in acid–base response to exercise between two groups contributed to the observed intergroup difference in P_{ETCO_2}-intercept (B), since exercise was performed at a relatively low intensity (below the ventilatory threshold, with no intergroup difference in plasma lactate) (Table 1).

Another important factor that could contribute to a decrease in the P_{ETCO_2}-intercept (B) during exercise is a change in the arterial-to-central difference in P_{CO_2}, which is primarily determined by changes in cerebral blood flow or cerebrovascular CO_2 reactivity (Peebles et al. 2007; Ainslie and Duffin 2009). In the previous study, we showed that an increase in cerebrovascular CO_2 reactivity during exercise compensated for an attenuated respiratory chemoreflex system controllability during exercise, especially under hypercapnic condition (Ogoh et al. 2008). Although the interaction between systemic and cerebral CO_2 controlling mechanisms during exercise was not examined in the present study, we speculate that intergroup differences in the control of cerebral blood flow and cerebrovascular CO_2 reactivity during exercise might have contributed, at least in part, to the observed differences.

To better understand the integrated characterization of the human chemoreflex system controlling ventilation using an equilibrium diagram, the interpretation and estimation of chemoreflex responsiveness using steady-state method should be addressed. Berkenbosch et al. (1989) and Mohan et al. (1999) demonstrated that the differences between rebreathing and steady-state affect the interpretation of results: the steady-state estimates are artefactually lower. Both Ainslie et al. (2008) and the review by Ogoh and Ainslie (2009) state that cerebral blood flow is increased in moderate exercise and this change is also affected by fitness; the gradient is reduced during exercise. This change with respect to testing at rest will produce an increase in slope during exercise compared to at rest. Whether or not this increase accounts for the whole of the change is unknown, but if it does then the increase in the controller gain (S) during exercise could well be artefactual. Indeed in Fig. 4a, taking only the two highest P_{CO_2} points where the gradient can be assumed to be minimized by the increased cerebral blood flow (Mohan et al. 1999), the two lines at rest and during exercise appear to be parallel.

Exercise-induced shift in the plant property

In the past, many researchers have explained the exercise-induced changes in plant property using the conventional metabolic hyperbola (Wasserman et al. 1986; Whipp and Pardy 1986). The equation that expresses the relation between $\dot{V}_E$ and P_{aCO_2} during exercise disregards the scaling factors representing ventilatory work-related CO_2 production. However, because ventilatory work-related CO_2 production occurs and V_D/V_T changes with variation in $\dot{V}_E$ in the "actual life" physiological system, we modified the conventional metabolic hyperbola to explain the exercise-induced changes in plant property (see Appendix). In the modified metabolic hyperbola [$P_{ETCO_2} = A/\dot{V}_E + C$], exercise-induced change in the plant property is characterized by an increase in A and a decrease in C. The increase in A may result from increases in basal metabolic demand (α value) and/or V_D/V_T (Appendix, Eq. 3). The decrease in C may result from decreases in V_D/V_T and/or metabolic cost of breathing (β value) (Appendix Eq. 3). V_D/V_T is unlikely to increase during exercise, because the exercise stimulus increases V_T but decreases V_D due to improved $\dot{V}_A/Q$ mismatch. β value probably decreases with reduced airway resistance, consequently reduced oxygen cost of breathing. Therefore, the increase in A may be attributed to the increase in basal metabolic demand, and the decrease in C to decreases in both V_D/V_T and β value.

Numerous reports have consistently shown that regular training induces a substantial reduction in $\dot{V}_E$ during exercise (Byrne-Quinn et al. 1971; Taylor and Jones 1979; Martin et al. 1979; Yerg et al. 1985; Casaburi et al. 1987b; Caillaud et al. 1993). The ventilatory requirement seems to be more reduced at higher exercise intensity level. Casaburi et al. (1987a, b) suggests that the reduced ventilatory response during exercise may be related to peripheral factors such as decreased blood lactate concentration, reduced CO_2 production caused by increased fatty acid metabolism, and other metabolite factors. In this study, however, exercise training does not affect the